Resolution Improvement of All-Optical Analog-to-Digital Conversion Employing Self-frequency Shift and Self-Phase-Modulation-Induced Spectral Compression

Takashi Nishitani, *Student Member, IEEE*, Tsuyoshi Konishi, *Member, IEEE*, and Kazuyoshi Itoh, *Member, IEEE*

***Abstract*—We demonstrate and investigate resolution improvement of optical quantization using soliton self-frequency shift (SSFS) and optical coding using optical interconnection for an all-optical analog-to-digital conversion (ADC). Incorporating spectral compression into the optical quantization allows us to improve the resolution bit according to the spectral compression ratio with keeping its throughput. The proposed scheme consists of optical quantization using SSFS and self-phase modulation (SPM) induced spectral compression and optical coding using optical interconnection based on a binary conversion table. In optical quantization, the powers of input signals are discriminated by referring to the center wavelengths after the SSFS. The compression of the spectral width allows us to emphasize the differences of their center wavelengths, and improve the number of resolution bits. Optical interconnection generates a bit-parallel binary code by appropriate allocation of a level identification signal, which is provided as a result of optical quantization. Experimental results show the eight periods transfer function, that means, the four read-out bit operation of the proposed scheme in binary code. Simulation results indicate that the proposed optical quantization has the potential of 100 GS/s and 4-b resolution, which could surpass the electrical bandwidth limitations.**

***Index Terms*—Optical analog-to-digital conversion, optical signal processing, soliton self-frequency shift (SSFS), self-phase modulation (SPM).**

I. Introduction

ANALOG-TO-DIGITAL conversion (ADC) has been investigated as a key interface technology in any electronic or photonic systems to convert continuous analog value of electrical or optical signals into discrete digital ones. Recent tremendous growths of the ultrawide-bandwidth applications such as advanced radar systems, optical communications, and real-time measurements encourage the demands of high-speed and high-resolution ADCs. State of the art electrical circuit technology realizes the high-resolution ADC whose resolution is ten or more bits at moderate sampling rate from megasamples per second (MS/s) to gigasamples per second (GS/s). In contrast, although a 25-GS/s, 3-b electrical ADC has been proposed [1], there is a unavoidable tradeoff between the sampling rate and the resolution bit due to electrical jitter of the sampling aperture and ambiguity of the comparator [2]–[4]. Optical approaches to the ADC provide many performance advantages over their electrical counterparts [3], [4]. The most effective advantage of optical approach is reducing jitter of sampling aperture [5] by the use of a stable mode-locked laser. Modern mode-locked lasers can produce high-frequency (>10 GHz) periodic sequences of an optical pulse with timing jitter significantly below that of electronic circuitry. Up to now, the timing jitter of an actively mode-locked laser has been measured to be 50 fs though under regulated conditions [6]. These low jitter characteristics of mode-locked lasers significantly improve the resolution bits of ADCs at the sampling rate under 10 GS/s. On the other hand, the ambiguity of electrical comparator prevents the improvement of resolution bits of ADCs at high sampling rate ADC over several tens gigasamples per second [2]. To overcome these problems due to electrical bandwidth limitation, several ADC architectures by using combination of optical demultiplexing and parallel electrical ADCs have been proposed [7]–[10]. In these approaches, however, the number of electrical ADC increases with increasing the desired sampling rate. Another related approach is the so-called time-streched ADC [11]–[14], which stretches the analog signal in time domain using a dispersion in a fiber. Although this approach realizes ultrahigh sampling rate at 480 GS/s [12], the throughput of the input signal is restricted by the stretch factor.

Meanwhile, to completely remove the electrical bandwidth limitation and pursue the high performance and high throughput ADC, optical approaches should also be applied to quantization and coding processes. For this purpose, several optical quantization and coding techniques have been proposed [15]–[25]. In these proposals, the use of nonlinear effect in fiber [16]–[20] is one promising approach, because it has ultrafast response speed and introduce various power dependent phenomena such as self-phase modulation (SPM), cross phase modulation, super continuum generation, Raman effect, etc. Previously, we have also proposed the optical quantization using soliton self-frequency shift (SSFS) in a fiber [18] and the several coding schemes [21], [23], [24] that support the proposed optical quantization, and confirmed 10 Gb/s error free operation [25], 3-b resolution [24], and high throughput operation over 100 Gb/s [25]. Since, however, the optical sampling using a low jitter mode-locked

Manuscript received November 1, 2007; revised December 14, 2007. This work was supported by the Research Fellowships of the Japan Society for the Promotion of Science for Young Scientists.

The authors are with the Graduate School of Engineering, Osaka University, Osaka 565-0871, Japan (e-mail: nishitani@photonics.mls.eng.osaka.u.ac.jp; konishi@mls.eng.osaka.u.ac.jp; itoh@mls.eng.osaka.u.ac.jp).

Color versions of one or more of the figures in this paper are available online at http://ieeexplore.ieee.org.

Digital Object Identifier 10.1109/JSTQE.2008.916251

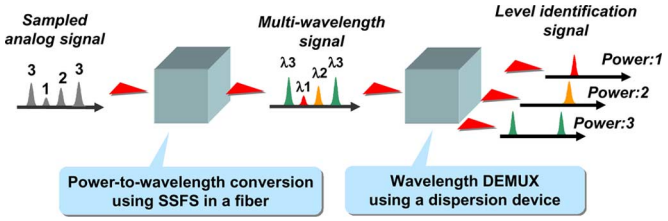

Fig. 1. Schematic diagram of the proposed optical quantization composed of power-to-wavelength conversion using SSFS in a fiber and wavelength demultiplexing using a dispersion device.

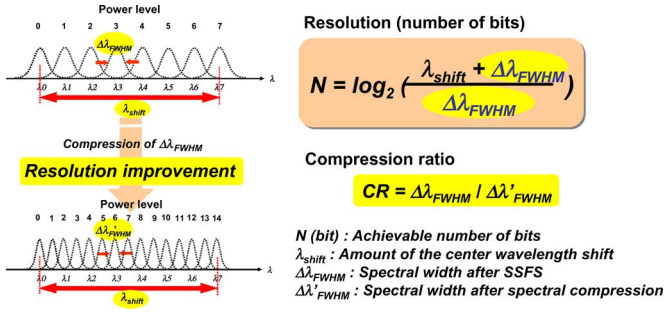

Fig. 2. Basic concept of the resolution improvement of the proposed optical quantization. The spectral compression enables to improve the resolution according to its compression ratio.

laser has the potential of four or more resolution bits at the sampling rate over 100 GS/s, the resolution improvement of optical quantization and optical coding should be investigated to pursue high-performance ADC. The resolution of the proposed all-optical ADC is in inverse proportion to a spectral width after the SSFS, but the spectral width should be enough wide to generate SSFS. To improve the resolution of the proposed all-optical ADC, the compression of the spectral width after the SSFS is one promising approach. Up to now, a spectral compression technique using SPM has been proposed for generation of ∼1 ps transform limited pulse from ∼100 fs pulse [26], and it is suitable for our purpose because the optical signal after the SSFS is a short pulse with several hundred femtosecond pulse width. In this paper, we propose the high-resolution all-optical ADC employing the SSFS and SPM-induced spectral compression, and demonstrate the 4-b all-optical ADC, which requires the eight periods transfer function.

II. Optical Quantization Scheme

A. Principle of Optical Quantization

The schematic diagram of the previously proposed optical quantization using the SSFS is shown in Fig. 1. It consists of two parts: power-to-wavelength conversion and wavelength demultiplexing. In power-to-wavelength conversion part, we use the SSFS in a fiber [27]. The SSFS is given by [28]

$$\kappa(Z) = -\frac{8}{15}\sigma_R \eta^4 Z \tag{1}$$

where κ is the center frequency of a soliton pulse, Z is a fiber length, σ_R is a coefficient of the self-induced Raman effect, and η is the amplitude of an input pulse. Equation (1) suggests that the amount of frequency shift increases in proportion to the fourth power of the amplitude and the fiber length. This power dependent feature is suitable for optical quantization. The operation principle of the proposed optical quantization is described as follows. The analog-sampled signal is propagated in a high-nonlinear fiber (HNLF) for the generation of the SSFS. After the SSFS, the center wavelength of each analog-sampled signal is shifted to a longer wavelength side. Since the amount of center wavelength shift increases with increasing a power of an analog-sampled signal, we can discriminate powers of analog-sampled signals referring to the center wavelengths. In wavelength demultiplexing part, we use a dispersion device such as arrayed waveguide grating (AWG). By placing an appropriate dispersion device after the SSFS, each different level identification signal of a power of an analog-sampled signal is provided at one specific port of the dispersion device. Consequently, we can realize optical quantization without any control of device.

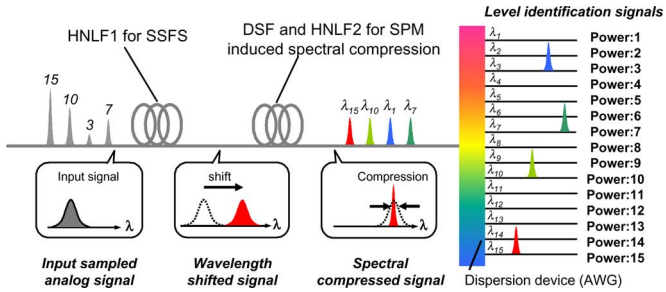

Fig. 3. Schematic diagram of the high-resolution optical quantization employing self-frequency shift and SPM-induced spectral compression.

B. Resolution Improvement of Optical Quantization Using SPM-Induced Spectral Compression

In the proposed optical quantization, the resolution, which is the achievable number of read-out bit N, is described by [18]

$$N = \log_2\left(\frac{\lambda_{\mathrm{shift}} + \Delta\lambda_{\mathrm{FWHM}}}{\Delta\lambda_{\mathrm{FWHM}}}\right) \tag{2}$$

where λ_{shift} and $\Delta\lambda_{\mathrm{FWHM}}$ are the amount of the center wavelength shift and the spectral width of the optical signal after the SSFS, respectively. From (2), we can confirm that the resolution of the proposed optical quantization is in inverse proportion to a spectral width $\Delta\lambda_{\mathrm{FWHM}}$ after the SSFS. However, the spectral width $\Delta\lambda_{\mathrm{FWHM}}$ should be enough wide to generate the SSFS. To improve the resolution of the proposed optical quantization, the compression of the spectral width $\Delta\lambda_{\mathrm{FWHM}}$ after SSFS is one promising approach, because it enables the improvement of the achievable bit number N according to the spectral compression ratio $CR(=\Delta\lambda_{\mathrm{FWHM}}/\Delta\lambda'_{\mathrm{FWHM}}$; see Fig. 2). Here, $\Delta\lambda'_{\mathrm{FWHM}}$ means the spectral width after the spectral compression. We focus attention on these points, and propose the high-resolution optical quantization scheme using the SSFS and spectral compression. The schematic diagram of the high-resolution optical quantization is shown in Fig. 3. Here, we try to use a spectral compression technique owing to negatively chirped

SPM after SSFS. In this scheme, first, the analog-sampled signal is propagated in an HNLF for the generation of the SSFS. The optical signal after the SSFS is propagated in a DSF for the generation of a negatively chirped pulse and HNLF for SPM. As a result, the spectral width of the optical signal after the SSFS is compressed owing to SPM-induced spectral compression. The spectral compressed signal is fed to an appropriate dispersion device such as AWG, and promptly output to one specific port corresponding to the input power as a level identification signal. Consequently, we can realize the optical quantization whose resolution is improved according to the spectral compression ratio.

III. Optical Coding Scheme

A. Coding Scheme for High-Resolution ADC

The optical coding scheme supports the optical quantization approach for the various applications. There are many coding schemes such as binary code, gray code, thermometer code, circular code, and one-to-*n* code, and their output formats are in either bit-serial format to a single port or bit-parallel one to many ports. The proposed optical quantization enables to output a single pulse at one specific port corresponding to a power of an input-sampled signal. This means that the proposed optical quantization can be regarded as one-to-*n* code coding scheme in a bit-parallel format. The one-to-*n* code is most flexible coding scheme, which allows us to extend in application of the all-optical ADC. We have proposed the several coding schemes that support the optical quantization approach as follows: 1) optical coding scheme using a pulse shaping technique that enables to output a thermometer-like code in a bit-serial format at a high chip rate over 600 Gchip/s to a single output port [21]; 2) optical coding scheme using optical delay line encoder that enables to output a binary or gray code in a bit-serial format at the chip rate in the range from several giga-chips per second to over a hundred giga-chips per second [23]; and 3) optical coding scheme using optical interconnection that enables to output binary or gray code in a bit-parallel format with keeping the input throughput [24], [25]. For the application to the optical format converter in high bit-rate optical communications, the former two coding schemes are suitable, because they enable to multiplex the optical data within a short time slot. Since, however, the chip rate of the bit-serial code increases with increasing the number of bits, they are not suitable for front-end applications, which require high-resolution bits and electrical detection by a photodiode. On the other hand, optical coding using optical interconnection is suitable for high-resolution front-end applications, because it enables to broadcast an optical signal to desired output ports in parallel with keeping the input throughput. For these reasons, we try to use the optical coding scheme using optical interconnection based on a binary conversion table to realize a high-resolution all-optical ADC.

B. Principle of Optical Coding Using Optical Interconnection

The schematic diagram of the optical coding scheme using optical interconnection based on a binary conversion table is shown in Fig. 4. It allows us to broadcast the level identification signal so as to provide multiple-bit binary code in a bit-parallel format. Here, the hexadecimal-to-binary conversion table for a 4-b binary code coding is shown in Table I as an example of a binary conversion table. The inputs $a0$–$a15$ are hexadecimal signals and the outputs $b1$–$b4$ are binary signals in Table I. From Table I, the outputs $b1$–$b4$ are described by the following:

$$\begin{aligned} b1 &= a1 + a3 + a5 + a7 + a9 + a11 + a13 + a15 \\ b2 &= a2 + a3 + a6 + a7 + a10 + a11 + a14 + a15 \\ b3 &= a4 + a5 + a6 + a7 + a12 + a13 + a14 + a15 \\ b4 &= a8 + a9 + a10 + a11 + a12 + a13 + a14 + a15. \end{aligned} \tag{3}$$

We can apply these equations to optical coding using optical interconnection so that a set of inputs and outputs may be corresponding to a power level of an analog-sampled signal and each bit in a 4-b binary signal, respectively. From (3), we can see that each bit in a 4-b binary code $b1$–$b4$ is formed by the combination of level identification signals $a1$–$a15$. Since the sum operation in (3) can be realized by optical interconnection, a level identification signal is broadcasted to appropriate output ports so as to provide a 4-b parallel binary code. Consequently, a multiple-bit binary code in a bit-parallel format corresponding to a power level of an analog-sampled signal can be provided to output ports. Since we can easily prepare optical interconnection patterns corresponding

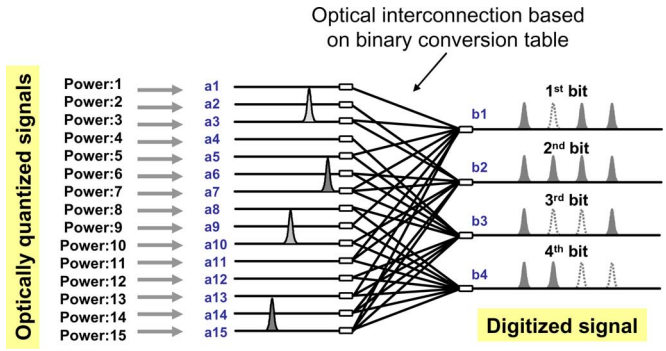

Fig. 4. Schematic diagram of the optical coding scheme using optical interconnection based on a binary conversion table. This figure shows the one example scheme for 4-b binary code coding scheme.

TABLE I
HEXADECIMAL-TO-BINARY CONVERSION TABLE FOR 4-B BINARY CODING

		Hexadecimal signal (Input)															
		a0	a1	a2	a3	a4	a5	a6	a7	a8	a9	a10	a11	a12	a13	a14	a15
binary signal (Output)	b1	0	1	0	1	0	1	0	1	0	1	0	1	0	1	0	1
	b2	0	0	1	1	0	0	1	1	0	0	1	1	0	0	1	1
	b3	0	0	0	0	1	1	1	1	0	0	0	0	1	1	1	1
	b4	0	0	0	0	0	0	0	0	1	1	1	1	1	1	1	1

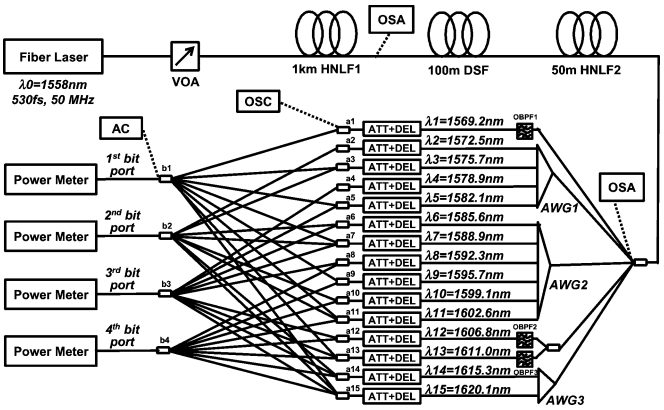

Fig. 5. Experimental set up of 4-b all-optical analog-to-digital conversion employing the SSFS and SPM-induced spectral compression. VOA: variable optical attenuator; HNLF: high nonlinear fiber; DSF: dispersion shifted fiber; OSA: optical spectrum analyzer; AWG: arrayed waveguide grating; OBPF: optical bandpass filter; DEL: delay line; ATT: fixed optical attenuator; AC: autocorrelator; OSC: oscilloscope.

to various codes, this coding technique can be used in many other coding schemes.

IV. Experimental Demonstration

To verify the operation of the proposed all-optical ADC, we demonstrate a 4-b all-optical ADC. In this demonstration, we set the output code as a binary code, which is the most basic and difficult coding scheme, because it requires the largest period transfer function in every coding scheme. The experimental set up is shown in Fig. 5. We used a short pulse irradiated from a fiber laser (IMRA America, Inc.) as a light source. The pulsewidth and the center wavelength were 0.53 ps and 1558 nm, respectively. We prepared a set of 15-level analog signals by adjusting the power of the input pulses using a variable optical attenuator (VOA). The peak powers of the input optical pulses were set as 16.1 W, 17.3 W, 18.5 W, 19.7 W, 21.0 W, 22.2 W, 23.4 W, 24.6 W, 25.5 W, 26.8 W, 28.1 W, 29.5 W, 30.8 W, 32.2 W, and 33.5 W. For the generation of SSFS, the input pulses were propagated in the 1 km HNLF1 (loss: $\alpha = 0.9$ dB/km; dispersion: $D = +7.2$ ps/nm·km; nonlinearity: $\gamma = 16$ /W/km; Sumitomo Electric Corporation, Ltd.). The optical pulses after the SSFS were propagated in the 100 m DSF (loss: $\alpha = 0.2$ dB/km; dispersion: $D = +2.0$ ps/nm·km; nonlinearity: $\gamma = 2.5$ /W/km) and the 50 m HNLF2 (loss: $\alpha = 0.6$ dB/km; dispersion: $D = +0.28$ ps/nm·km; nonlinearity: $\gamma = 9.0$ /W/km; Sumitomo Electric Corporation, Ltd.) for SPM-induced spectral compression. Each optical pulse after the SSFS and SPM-induced spectral compression was duplicated and fed to AWG1, 3 (200 GHz spacing; NTT Electronics Corporation, Ltd.), AWG2 (100 GHz spacing; ANDevice, Inc.), and 0.7 nm optical bandpass filters (OBPFs; OptQuest Corporation, Ltd.) being set for each center wavelength after the SSFS. To synchronize the timing and equalize the power of level identification signals, we adjusted the time delays and powers in advance using optical delay lines and optical attenuators placed at each output port of dispersion devices. Since the output ports $a1$–$a15$ of dispersion devices were connected by optical couplers based on a hexadecimal-to-binary conversion table, each bit in a 4-b binary code was output to the corresponding output port $b1$–$b4$. We measured the transfer functions of the output signals at each output port $b1$–$b4$ to confirm the operation of 4-b ADC. Experimental results of the output spectrums after the SSFS are shown in Fig. 6. From Fig. 6, we can confirm that the center wavelengths of optical pulses are successfully shifted depending on the input peak power, and each spectrum distribution has a single spectral peak. Since, however, the spectral distribution was overlapped each other, it is difficult to discriminate the power level by referring to the difference of the center wavelength before spectral compression. Experimental results of the output spectrums after the SSFS and SPM-induced spectral compression are shown in Fig. 7.

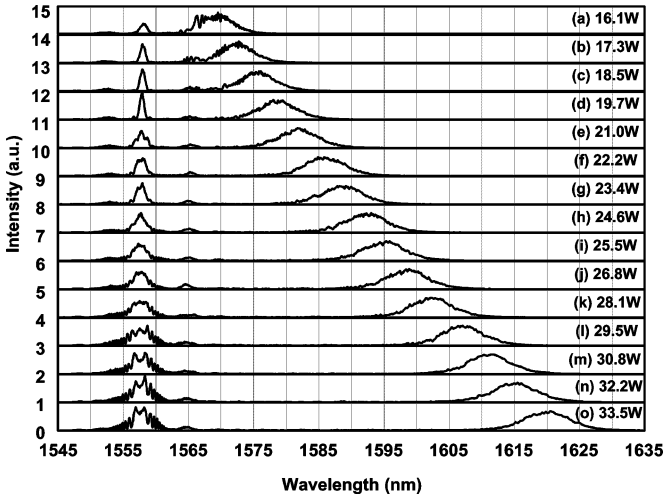

Fig. 6. Experimental results of the output spectrums after propagating in HNLF1 at different input peak powers. (a) 16.1 W. (b) 17.3 W. (c) 18.5 W. (d) 19.7 W. (e) 21.0 W. (f) 22.2 W. (g) 23.4 W. (h) 24.6 W. (i) 25.5 W. (j) 26.8 W. (k) 28.1 W. (l) 29.5 W. (m) 30.8 W. (n) 32.2 W. and (o) 33.5 W.

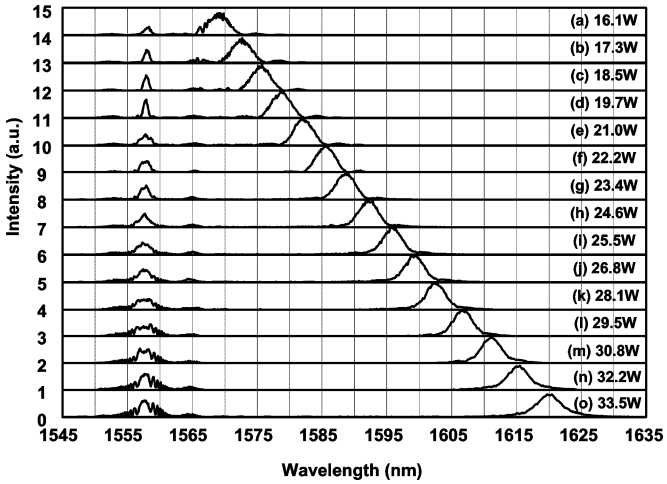

Fig. 7. Experimental results of the output spectrums after propagating in HNLF1, DSF, and HNLF2 at different input peak powers. (a) 16.1 W. (b) 17.3 W. (c) 18.5 W. (d) 19.7 W. (e) 21.0 W. (f) 22.2 W. (g) 23.4 W. (h) 24.6 W. (i) 25.5 W. (j) 26.8 W. (k) 28.1 W. (l) 29.5 W. (m) 30.8 W. (n) 32.2 W. and (o) 33.5 W.

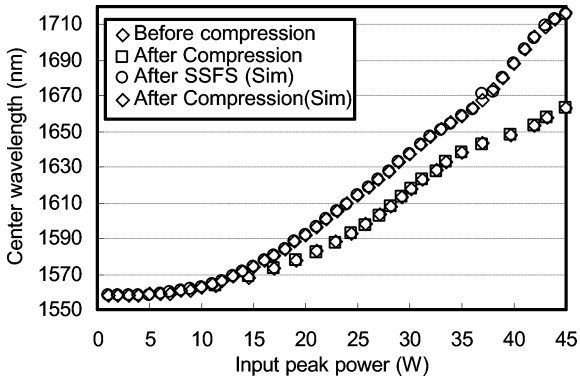

Fig. 8. Experimental and simulation results of the relationships between the center wavelengths and the input peak powers before and after the spectral compression.

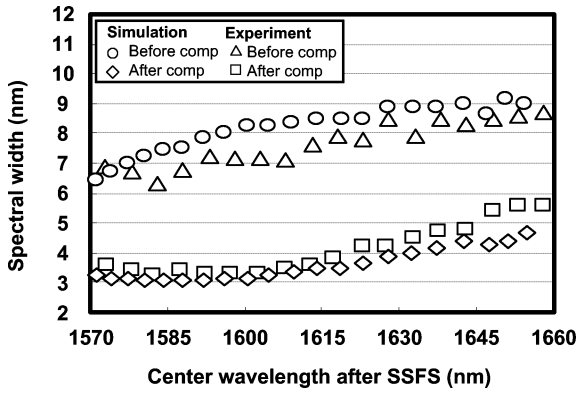

Fig. 9. Experimental and simulation results of the relationships between the spectral widths and the center wavelengths before and after the spectral compression.

From Fig. 7, we can confirm that the spectral widths of optical pulses after the SSFS are successfully compressed by the SPM-induced spectral compression, and the overlapped spectral component can be reduced. Experimental and simulation results of the relationship between the center wavelength and the input peak power before and after the spectral compression are shown in Fig. 8. From Fig. 8, we can confirm that the center wavelength was shifted depending on the input peak power, and it was not changed after the SPM-induced spectral compression. Fig. 9 shows the experimental and simulation results of the relationship between the spectral width and the center wavelength before and after the spectral compression. From Fig. 9, we can confirm the compression ratio of 2–1 without wavelength dependency. These results indicate that we can achieve the double resolution of optical quantization or one resolution bit improvement by the use of SPM-induced spectral compression. From these results, we set the pass wavelengths of dispersion devices as 1569.2 nm, 1572.5 nm, 1575.7 nm, 1578.9 nm, 1582.1 nm, 1585.6 nm, 1588.9 nm, 1592.3 nm, 1595.7 nm, 1599.1 nm, 1602.6 nm, 1606.8 nm, 1611.0 nm, 1615.3 nm, and 1620.1 nm. Fig. 10 shows the temporal waveforms of output signals measured by an oscilloscope with 53 GHz bandwidth photo diode (86100 A and 86116 A; Agilent Technologies, Inc.)

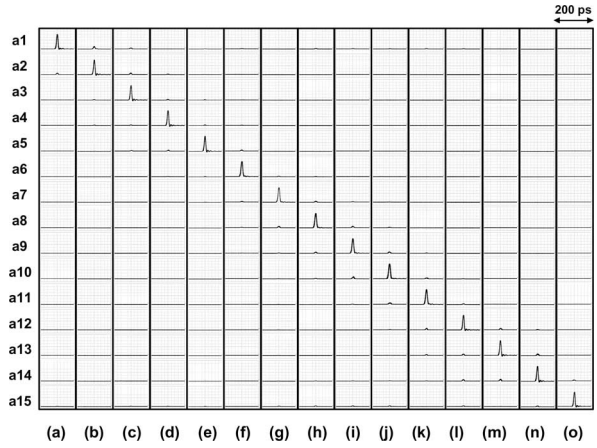

Fig. 10. Experimental results of the measured temporal waveforms detected by 53 GHz bandwidth PD at each output port $a1$–$a15$ of dispersion devices at different input peak powers. (a) 16.1 W. (b) 17.3 W. (c) 18.5 W. (d) 19.7 W. (e) 21.0 W. (f) 22.2 W. (g) 23.4 W. (h) 24.6 W. (i) 25.5 W. (j) 26.8 W. (k) 28.1 W. (l) 29.5 W. (m) 30.8 W. (n) 32.2 W. and (o) 33.5 W.

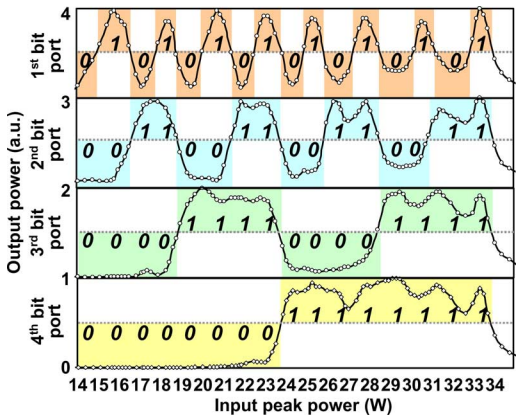

Fig. 11. Experimental results of the measured transfer functions of each output port $b1$–$b4$.

at each output port $a1$–$a15$ of dispersion device when input powers are ideally chosen without quantization errors. From Fig. 10, the level identification signals were output from the one specific port of dispersion device according to the input peak power. Fig. 11 shows the measured transfer function of each output port $b1$–$b4$ by power meters (AQ 8201-22; Yokogawa Electric Corporation, Ltd.). From Fig. 11, we can successfully confirm the eight periods transfer function at the first bit port $b1$. However, as can be seen from Fig. 11, when the power of an input pulse lies on the edges of the wavelength bands, it is regarded as a quantization error. To solve this problem, we consider that the application of the optical binary thresholding technique or optical regeneration technique to each output digital signal should be required. These optical thresholding or the regeneration technique enables to improve the SNR of the proposed scheme and makes it more practical one. From the experimental results of autocorrelation measurements by an autocorrelator (Alnair Laboratories Corporation, Ltd.), a single pulse whose pulse width ranges from 3.8 to 7.7 ps estimated by the autocorrelation

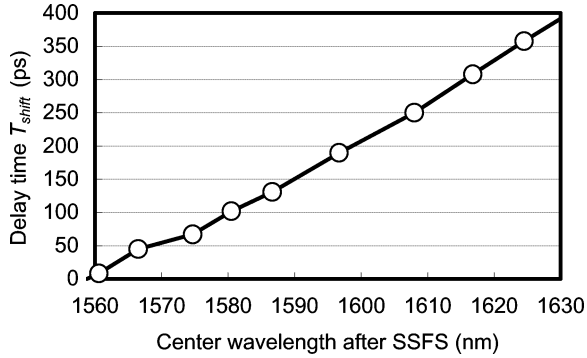

Fig. 12. Experimental results of the relationship between the center wavelength after the SSFS and the relative delay time after propagating HNLF1 (loss: α =0.9 dB/km; dispersion: $D = +7.2$ ps/nm·km; nonlinearity: $\gamma = 16$/W/km; Sumitomo Electric Corporation, Ltd.).

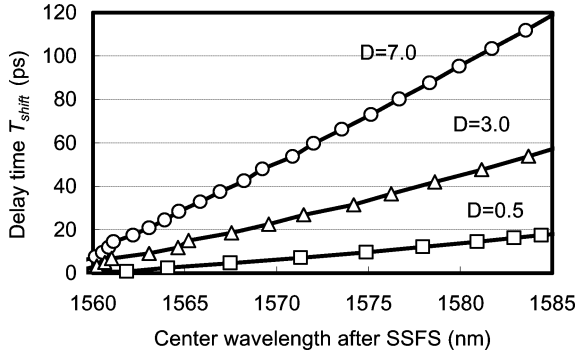

Fig. 13. Simulation results of the relationship between the center wavelength after the SSFS and the delay time by changing the dispersion D of the HNLF in the case of the fiber length $Z = 1$ km.

trace, was output as each bit in a multiple-bit binary number at the appropriate output port corresponding to the input peak power. From these results, we have successfully demonstrated the 4-b optical quantization and coding. In this experiment, we chose the difficult binary coding scheme, because we prove the flexibility of the proposed optical coding method using optical interconnection. We can demonstrate other coding schemes such as gray code coding scheme by preparing appropriate optical interconnection pattern.

V. Discussion

A. Throughput of the Proposed Optical Quantization

The requirement for high-sampling rate optical ADC is the high-speed responsibility and the feasibility for high-throughput optical signals after optical sampling process. The response speed of the proposed all-optical ADC is very fast, about few femtoseconds, because it depends on the response speed of Raman effect for self-frequency shift. On the other hand, the throughput is limited by the walk-off issue caused by wavelength dispersion in fiber. Since the center wavelengths of input signals are shifted to longer wavelength side owing to SSFS, the optical signals after the SSFS have each different propagation speed and delays depending on corresponding center wavelengths. Fig. 12 shows the experimental results of the relationship between the center wavelength and relative delay time after propagating in HNLF1 (loss: $\alpha = 0.9$ dB/km; dispersion: $D = +7.2$ ps/nm·km; nonlinearity: $\gamma = 16$ /W/km; Sumitomo Electric Corporation, Ltd.) for the generation of SSFS. From this result, the delay time increases with increasing the amount of the center wavelength shift. In the experiment of 4-b all-optical ADC, because the center wavelength after the SSFS ranges from 1569 to 1620 nm, the delay time is 330 ps from Fig. 12. This delay time indicates that the throughput of the input-sampled analog signal is up to 3 Gb/s at 4-b resolution. To pursue the high-performance ADC, the further improvement of the throughput should be investigated. Here, the throughput TP of the proposed all-optical ADC described by

$$\mathrm{TP} = \frac{1}{T_{\mathrm{shift}}} \propto \frac{1}{\lambda_{\mathrm{shift}} DZ} \tag{4}$$

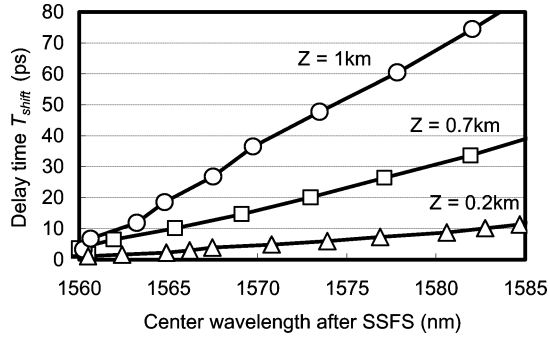

Fig. 14. Simulation results of the relationship between the center wavelength after the SSFS and the delay time by changing the fiber length Z of the HNLF in the case of the dispersion $D = 3.0$ ps/nm·km.

where T_{shift} is the relative delay time of the optical signal after the SSFS, and D and Z are the dispersion and the fiber length of an HNLF for the generation of SSFS. From (4), the throughput of the proposed system is inverse proportion to the dispersion and fiber length of an HNLF for the generation of SSFS. To verify the high-throughput operation by the optimization of an HNLF, we executed the numerical simulation of pulse propagation in a fiber using a split-step Fourier method (SSFM). In this simulation, we used a transform limited sech^2 pulse. The center wavelength and pulsewidth were 1558 nm and 0.53 ps, respectively. For the generation of SSFS, the optical pulse was propagated in an HNLF (loss: $\alpha = 0.9$ dB/km, $\gamma = 16$ /W/km). We investigated the relationship between the center wavelength and the delay time after the SSFS by changing the dispersion D and the fiber length Z of an HNLF. Fig. 13 shows the simulation results of the relationship between the center wavelength and the delay time T_{shift} by changing the dispersion D in the case of the fiber length $Z = 1$ km. From Fig. 13, the delay time could be decreased by the use of a small dispersion fiber. Fig. 14 shows the simulation results of the relationship between the center wavelength and the delay time by changing the fiber length Z in the case of the dispersion $D = 3.0$ ps/nm·km. From Fig. 14, the delay time could be decreased by the use of a shorter fiber. We have already demonstrated the high-throughput all-optical ADC with 2-b resolution at 100 Gb/s using an HNLF whose dispersion and

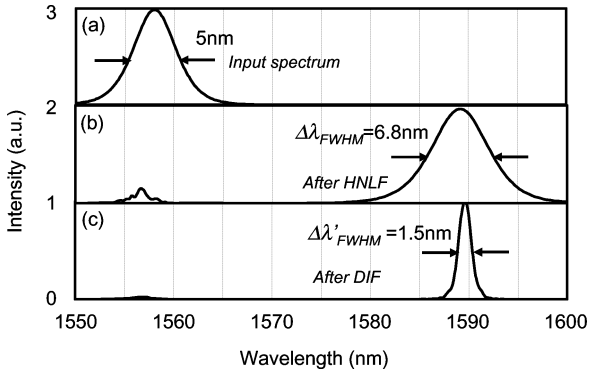

Fig. 15. Simulation results of the spectral evolution of an input pulse propagating in fibers in the case of the input peak power 21 W. (a) Input spectrum. (b) Output spectrum after propagating in HNLF for generation of SSFS. (c) Output spectrum after propagating in DIF for spectral compression.

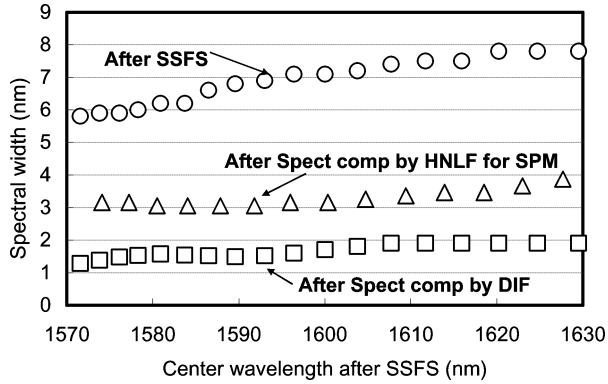

Fig. 16. Simulation results of the relationship between the center wavelength after the SSFS and the spectral width before and after the spectral compression using HNLF and DIF.

fiber length are $D = -0.06$ ps/nm·km and $Z = 10$ m [25]. This demonstration indicates that we could realize high-throughput all-optical ADC over 100 GS/s by the optimization of an HNLF for the generation of SSFS.

B. Resolution of the Proposed Optical Quantization

The resolution of the proposed all-optical ADC is described by (2). From experimental results in Figs. 8 and 9, we can confirm that the amount of the center wavelength shift $\lambda_{\rm shift}$ and the average spectral width after the SSFS and spectral compression $\Delta\lambda'_{\rm FWHM}$ are over 150 and 4 nm, respectively. These results give a promise of greater 5.2-b resolution. For further improvement of the resolution bit, the optimization of a fiber for spectral compression is one promising approach. The spectral compression using a dispersion increasing fiber (DIF) [29] is considered as one of the most suitable methods, because it enables to effectively compress the spectral width with an adiabatic process. To confirm the availability of a DIF for spectral compression, we executed a numerical demonstration. In the numerical demonstration, we used a transform limited sech^2 pulse. The center wavelength and pulsewidth were 1558 nm and 0.53 ps, respectively. For the generation of SSFS, the optical pulse was propagated in an HNLF (loss: $\alpha = 0.9$ dB/km; dispersion: $D = +7.2$ ps/nm·km; nonlinearity: $\gamma = 16$ /W/km). The optical signal after the SSFS was propagated in a 1 km DIF (loss: $\alpha = 0.7$ dB/km; dispersion: $D = +2$ to $+7$ ps/nm·km; nonlinearity: $\gamma = 3.7$ /W/km) for spectral compression. Fig. 15 shows the simulation results of the spectral evolution of an input pulse propagating in fibers in the case of the input peak power 21 W. From Fig. 15, we can confirm the spectral compression of the optical signal after the SSFS by propagating in a DIF. Fig. 16 shows the simulation results of the relationship between the center wavelength after the SSFS and the spectral width before and after the spectral compression using an HNLF for SPM and a DIF. From Fig. 16, we can confirm that the spectral compression ratio of 4 to 1, which is twice as many as by using an HNLF for SPM, was obtained by using a DIF for spectral compression. These results indicate that we could achieve one more bit resolution improvement by using a DIF than using an HNLF for SPM.

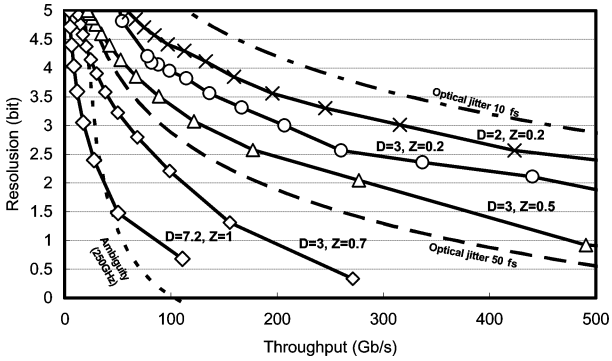

Fig. 17. Simulation results of the resolution bit of the proposed all-optical ADC as a function of its throughput by changing D and Z.

C. Performance of the Proposed Optical Quantization

The performances of ADCs are defined by the product of sampling rate and resolution bits [2]. The performance of the proposed all-optical ADC is restricted by some parameters as seen in earlier discussion about the throughput and the resolution bits. From (2) and (4), the relationship between the throughput TP and resolution bit N is described by

$$N \propto \log_2\left(\frac{1}{DZ\Delta\lambda'_{\rm FWHM}\,\mathrm{TP}} + 1\right). \tag{5}$$

From (6), we can improve the performance of the proposed all-optical ADC by decreasing the dispersion D, fiber length Z, and the spectral width $\Delta\lambda'_{\rm FWHM}$. Fig. 17 shows the simulation results of the resolution bits of the proposed all-optical ADC as a function of its throughput by changing D and Z. In this simulation, we set $\Delta\lambda'_{\rm FWHM}$ as 1.5 nm assuming that we use a DIF for spectral compression. The theoretical limitations of the ambiguity of an electrical comparator at 250 GHz bandwidth and the optical sampling jitters of 10 and 50 fs are also shown in Fig. 17. In the case of $D = 7.2$ and $Z = 1$, which are the

same parameters as used in the experiment, we can successfully surpass the resolution limit of the ambiguity of the electrical comparator at the throughput over 35 Gb/s. In addition, we can confirm that, the less the dispersion and fiber length of an HNLF become, the more the TP and N of the proposed all-optical ADC become. From these results, the proposed all-optical ADC has the potential of high-performance operation over 100 GS/s, 4-b resolution by the optimization of fibers for the SSFS and spectral compression. This performance drastically surpasses the electrical counterpart.

VI. Conclusion

We have proposed optical quantization employing self-frequency shift and SPM-induced spectral compression and optical coding using optical interconnection for a high-resolution all-optical ADC. From experimental results, we confirmed the eight periods transfer function, that means, the four read-out bit operation of the proposed scheme in binary code. Simulation results indicated that the resolution of the proposed scheme could surpass the resolution limit of the several tens gigasamples per second electrical ADC, and further resolution and throughput improvement over 4 b and 100 Gb/s are expected by optimizing HNLFs for the SSFS and SPM-induced spectral compression.

References

[1] H. Nosaka, M. Nakamura, K. Sano, K. Kurishima, T. Shibata, and M. Muraguchi, "A 24-Gsps 3-bit nyquist ADC using HBTs for DSP-based electronic dispersion compensation," *IEICE Trans. Electron.*, vol. E88-C, no. 6, pp. 1225–1232, Jun. 2005.

[2] R. H. Walden, "Analog-to-digital converter survey and analysis," *IEEE J. Sel. Areas Commun.*, vol. 17, no. 4, pp. 539–550, Apr. 1999.

[3] G. C. Valley, "Photonic analog-to-digital converters," *Opt. Exp.*, vol. 15, no. 5, pp. 1955–1982, Mar. 2007.

[4] B. L. Shoop, *Photonic Analog-to-Digital Conversion*. Berlin, Germany: Springer-Verlag, 2001.

[5] P. W. Juodawlkis, J. C. Twichell, G. E. Betts, J. J. Hargreaves, R. D. Younger, J. L. Wasserman, F. J. O'Donnell, K. G. Ray, and C. Williamson, "Optically sampled analog-to-digital converters," *IEEE Trans. Microw. Theory Tech.*, vol. 49, no. 10, pp. 1840–1853, Oct. 2001.

[6] P. W. Juodawlkis, J. C. Twichell, J. L. Wasserman, G. E. Bets, and R. C. Williamson, "Measurement of mode-locked laser timing jitter by use of phase-encoded optical sampling," *Opt. Lett.*, vol. 26, no. 5, pp. 289–291, 2001.

[7] W. C. Black and D. A. Hodges, "Time interleaved converter arrays," *IEEE J. Solid-State Circuits*, vol. SC-15, no. 12, pp. 468–470, Dec. 1980.

[8] J. T. R. Clark and M. L. Dennis, "Toward a 100-GSample/s photonic A-D converter," *IEEE Photon. Technol. Lett.*, vol. 13, no. 3, pp. 236–238, Mar. 2001.

[9] A. Yariv and R. G. Koumans, "Time interleaved optical sampling for ultrahigh speed A/D conversion," *Electron. Lett.*, vol. 34, no. 21, pp. 2012–2013, Oct. 1998.

[10] P. Rabiei and A. F. J. Levi, "Analysis of hybrid optoelectronic WDM ADC," *J. Lightw. Technol.*, vol. 18, no. 9, pp. 1264–1270, Sep. 2000.

[11] Y. Han and B. Jalali, "Photonic time-stretched analog-to-digital converter: Fundamental concept and practical considerations," *J. Lightw. Technol.*, vol. 21, no. 12, pp. 3085–3103, Dec. 2003.

[12] Y. Han, O. Boyraz, and B. Jalali, "Ultrawide-band photonic time-stretch A/D converter employing phase diversity," *J. Lightw. Technol.*, vol. 53, no. 4, pp. 1404–1408, Jul. 2005.

[13] J. Chou, G. A. Sefler, J. Conway, G. C. Valley, and B. Jalali, "4-channel continuous-time 77 GSa/s ADC using photonic bandwidth compression," in *Proc. IEEE Int. Top. Meet. Microw. Photon.*, Oct., 2007, pp. 54–57.

[14] J. Chou, O. Boyraz, D. Solli, and B. Jalali, "Femtosecond real-time single-shot digitizer," *Appl. Phys. Lett.*, vol. 91, no. 16, pp. 161105–161107, Oct. 2007.

[15] H.F. Taylor, "An electro-optic analog-to-digital converter," in *Proc. IEEE*, vol. 63, no. 10, pp. 1524–1525, Oct. 1975.

[16] J.-M. Jeong and M. E. Marhic, "All-optical analog-to-digital and digital-to-analog conversion implemented by a nonlinear fiber interferometer," *Opt. Commun.*, vol. 91, no. 1–2, pp. 115–122, Jul. 1992.

[17] P. P. Ho, Q. Z. Wang, J. Chen, Q. D. Liu, and R. R. Alfano, "Ultrafast optical pulse digitization with unary spectrally encoded cross-phase modulation," *Appl. Opt.*, vol. 36, no. 5, pp. 3425–3429, May 1997.

[18] T. Konishi, K. Tanimura, K. Asano, Y. Oshita, and Y. Ichioka, "All-optical analog-to-digital converter by use of self-frequency shifting in fiber and a pulse-shaping technique," *J. Opt. Soc. Am. B*, vol. 19, no. 12, pp. 2817–2823, Nov. 2002.

[19] S. Oda, A. Maruta, and K. Kitayama, "All-optical quantization scheme based on fiber nonlinearity," *IEEE Photon. Technol. Lett.*, vol. 16, no. 2, pp. 587–589, Feb. 2004.

[20] K. Ikeda, J. M. Abdul, H. Tobioka, T. Inoue, S. Namiki, and K. Kitayama, "Design considerations of all-optical A/D conversion: Nonlinear fiber-optic sagnac-loop interferometer-based optical quantizing and coding," *J. Lightw. Technol.*, vol. 24, no. 7, pp. 2618–2628, Jul. 2006.

[21] T. Nishitani, T. Konishi, and K. Itoh, "Integration of a proposed all-optical analog-to-digital converter using self-frequency shifting in fiber and a pulse-shaping technique," *Opt. Rev.*, vol. 12, no. 3, pp. 237–241, May/Jun. 2005.

[22] J. Stigwall and S. Galt, "Demonstration and analysis of a 40 gigasample/s interferometric analog-to-digital converter," *J. Lightw. Technol.*, vol. 24, no. 3, pp. 1247–1256, Mar. 2004.

[23] T. Nishitani, T. Konishi, and K. Itoh, "All-optical analog-to-digital conversion using optical delay line encoders," *IEICE Trans. Electron.*, vol. E-90C, no. 2, pp. 479–480, Feb. 2007.

[24] T. Nishitani, T. Konishi, and K. Itoh, "Optical coding scheme using optical interconnection for high sampling rate and high resolution photonic analog-to-digital conversion," *Opt. Exp.*, vol. 15, no. 24, pp. 15812–15817, Nov. 2007.

[25] T. Nishitani, T. Konishi, and K. Itoh, "All-optical M-ary ASK signal demultiplexer based on photonic analog-to-digital conversion," *Opt. Exp.*, vol. 15, no. 25, pp. 17025–17031, Dec. 2007.

[26] B. R. Washburn, J. A. Buck, and S. E. Ralph, "Transform-limited spectral compression due to self-phase modulation in fibers," *Opt. Lett.*, vol. 25, no. 7, pp. 445–447, Apr. 2000.

[27] J. P. Gordon, "Theory of the soliton self-frequency shift," *Opt. Lett.*, vol. 11, no. 10, pp. 662–664, Oct. 1986.

[28] A. Hasegawa and Y. Kodama, *Solitons in Optical Communications*. Oxford, U.K.: Oxford Univ. Press, 1995.

[29] C. Xu and X. Liu, "Photonic analog-to-digital converter using soliton-frequency shift and interleaving spectral filters," *Opt. Lett.*, vol. 28, no. 6, pp. 986–988, May 2003.

Takashi Nishitani (S'06) received the B.E. degree in applied physics and the M.E. degree in material and life science, in 2003 and 2005, respectively, from Osaka University, Osaka, Japan, where he is currently working toward the Ph.D. degree in advanced science and biotechnology.

His current research interests include free space optics, optical signal processing, and nonlinear optical phenomena.

Mr. Nishitani is a member of the Japan Society of Applied Physics (JSAP), the Institute of Electronics, Information, and Communication Engineers (IEICE), and the Optical Society of Japan (OSJ).

Tsuyoshi Konishi (M'99) received the B.E., M.E., and Dr.E. degrees in applied physics from Osaka University, Osaka, Japan, in 1991, 1993, and 1995, respectively.

Since 1996, he has been with the Graduate School of Engineering (GSE), Osaka University, earlier as an Assistant Professor, and currently, as an Associate Professor in the Division of Advanced Science and Biotechnology. His current research interests include ultrafast optical signal processing.

Dr. Konishi is a member of the Institute of Electronics, Information, and Communication Engineers, the Japan Society of Applied Physics, the Optical Society of Japan (OSJ), the Optical Society of America (OSA), and the International Society for Optical Engineering (SPIE).

Kazuyoshi Itoh (M'00) received the B.Eng. and M.Eng. degrees from Osaka University, Osaka, Japan, in 1971 and 1975, respectively, and the D.Eng. degree from Hokkaido University, Sapporo, Japan, in 1984, all in applied physics.

From 1971 to 1972, he was with Nippon Kokan K.K. From 1975 to 1978, he was with the Matsushita Electric Industrial Company, Ltd., Osaka. During 1978, he was with Hokkaido University. During 1986, he was with the Department of Applied Physics, Faculty of Engineering, Osaka University. Since 1995, he has been in the Division of Advanced Science and Biotechnology, Graduate School of Engineering, Osaka University, as a Professor, where he has been engaged in research on optical coherence, optical information processing, and digital and nonlinear image processing. His current research interests include ultrashort optical pulses to biophotonics, optical signal processing, and material processing.

Dr. Itoh was the Editor-in-Chief of the *Japanese Journal of Optics* from 1997 to 1999 and as an Editor-in-Chief of the *Japanese Journal of Applied Physics* from 2002 to 2004.